

PERIODICO di MINERALOGIA  
established in 1930

An International Journal of  
MINERALOGY, CRYSTALLOGRAPHY, GEOCHEMISTRY,  
ORE DEPOSITS, PETROLOGY, VOLCANOLOGY  
and applied topics on Environment, Archeometry and Cultural Heritage

Special Issue in memory of Sergio Lucchesi

## The peculiar crystal-chemistry of phlogopite from metasomatized peridotites: evidence from laboratory and nature

Paola Comodi<sup>1,\*</sup>, Sabrina Nazzareni<sup>1</sup>, Patrizia Fumagalli<sup>2</sup> and Gian Carlo Capitani<sup>3</sup>

<sup>1</sup>Dipartimento di Scienze della Terra, Università di Perugia, Italy

<sup>2</sup>Dipartimento di Scienze della Terra, Università di Milano, Italy

<sup>3</sup>Dipartimento di Scienze Geologiche e Geotecnologie, Università di Milano Bicocca, Italy

\*Corresponding author: [comodip@unipg.it](mailto:comodip@unipg.it)

### Abstract

Experimental petrology suggested that phlogopite has a peculiar mineral chemistry at high pressure: excess of Si coupled with a decrease in <sup>IV</sup>Al and deficiency in K+Na. This *K-edenite* exchange,  $\square^{\text{XII}}\text{Si}(\text{K}+\text{Na})_{-1}\text{Al}_{-1}$ , where  $\square^{\text{XII}}$  is a vacancy in the interlayer, should imply that phlogopites incorporate significant amount of talc component. At high pressure conditions, however, in a fluid saturated system, a talc component might translate into a 10 Å phase component, being the latter phase the product of the reaction talc + H<sub>2</sub>O = 10 Å phase occurring at  $P = 4 - 5$  GPa and at  $T = 600-700$  °C.

We aim to study the structure of natural and synthetic phlogopites showing this peculiar mineral chemistry. Samples were analysed by single-crystal X-ray diffraction, powder X-ray diffraction with full profile fitting, EMP, SIMS, TEM and Mössbauer spectroscopy. The natural samples were recovered from spinel and garnet wedge peridotites of the Ulten Zone Eastern Italian Alps, (Italy), whereas synthetic ones were obtained from high pressure synthesis in a K-doped lherzolite system. The single crystal X-ray refinements of natural phlogopites, together with the EMP analysis, showed two coupled substitutions: *Tschermak* ( $\text{Si} + \text{Mg} = \text{IVAl} + \text{VIAl}$ ) and *talc* exchanges ( $\square + \text{Si} = \text{K} + \text{Al}$ ), with no octahedral vacancies. The Rietveld refinement of the synthetic samples confirmed the ipersilicic character and K deficiency found with EMPA and SIMS analysis. The *c* lattice parameter of both synthetic and natural phlogopites positively correlates with the increase of vacancies at the interlayer site, pointing toward the *c* lattice parameter of the 10Å phase. The tetrahedral  $\alpha$  rotation angle of natural phlogopites was about 9°, lower than that expected by *Tschermak* substitution. The present data indicate that the 10 Å phase component, instead of the *talc component*, stabilizes the phlogopite structure by reducing the  $\alpha$  rotation under high pressure condition. This increases the pressure conditions needed to reach the upper limit value for the tetrahedral rotation.

*Key words:* phlogopite; 10 Å phase; single crystal X-ray refinements; EMPA; SIMS.

## Introduction

Phlogopites and amphiboles are expected to play an important role in mass transport and metasomatism occurring both along the subducting slab at the mantle-slab interface and within the mantle wedge. Their occurrence has been reported in several mantle xenoliths and ultramafic rocks (e.g. Ulten Zone, Tonale Nappe, Italy, Morten et al., 2004; Bardane region, Western Norway, van Roermund, 2002; Kokchetav Massif, Sobolev and Shatsky, 1990; Dabie Shan region, Zheng et al., 2005). The presence of hydrous and carbonates phases, (Comodi et al., 1990), is an evidence for devolatilization processes occurring in the subducted lithosphere, leading to a continuous C-O-H fluid release, which metasomatizes the overlying mantle wedge (e.g. Poli and Schmidt, 2002). In addition the mass transfer between crustal slab and mantle wedge and the thermophysical parameters during the interaction ( $T$ ,  $P$ ,  $f_{H_2}$ ,  $f_{O_2}$ ) can be studied through a detailed crystal-chemical analysis of hydrous phases generally found enclosed in orogenic belt.

The stability of phlogopite in mantle assemblages has been widely investigated in simple systems (Kushiro et al., 1967; Trønnes, 2002; Kushiro, 1970; Modreski and Boettcher, 1973; Luth, 1997; Sudo and Tatsumi, 1990) and in more complex systems approaching natural peridotites (i.e. Fumagalli et al., 2009 and references therein). In lherzolites, phlogopite is stable up to 6.0-6.5 GPa at 1000 °C and shows a peculiar crystal chemistry: depending on pressure, the increase of Si is associated to a decrease in Al and interlayer cations (K firstly and Na). The *K-edenite* exchange,  $\square^{XII}Si(K+Na)_{-1}Al_{+1}$ , was hypothesized on a chemical basis (Fumagalli et al., 2009), suggesting a pressure dependent incorporation of a talc component in high pressure phlogopites. Furthermore in fluid saturated system, due to the reaction  $talc + H_2O = 10 \text{ \AA phase } (Mg_3Si_4O_{10} \times n H_2O)$  at  $P = 4-6$

GPa and  $T = 600-700 \text{ }^\circ\text{C}$ , the talc substitution might translate into the incorporation of a 10 Å phase component (Pawley and Wood, 1995).

This paper intends to investigate the crystal structure and crystal chemistry of synthetic and natural phlogopites found in metasomatized peridotitic systems, to evaluate the extension of the *K-edenite* exchange (or *talc substitution*), its effect on the crystal structure and whether the 10 Å phase or talc represents the end member of this coupled substitution.

This was achieved by a multi-methodic approach: X-ray diffraction (on single-crystal for the natural samples and on powder for the synthetic samples), Electron MicroProbe Analysis (EMPA), Transmission Electron Microscopy (TEM), and Secondary Ion Mass Spectrometry (SIMS). To better constrain the crystal chemistry of the natural samples Mössbauer spectroscopy was also carried out.

## Samples description

### *Natural samples*

Natural samples were selected from peridotitic bodies of the Ulten Zone unit (Eastern Alps, Italy). They are believed to represent a subcontinental mantle wedge, which underwent metasomatic enrichments during the subduction of a crustal slab in Variscan times (Obata and Morten, 1987).

Metasomatic minerals in the Ulten peridotites are amphiboles  $\pm$  phlogopite  $\pm$  chlorite, and rarely apatite and carbonate. Pargasitic amphiboles are the most abundant hydrous phase (Obata and Morten, 1987). Phlogopites-rich bands characterise the contacts between peridotites and migmatites (Godard et al., 1996) or pyroxenitic veins, i.e. garnet-websterite (Morten and Obata, 1990). In both cases, phlogopite extends up to few tenths of centimeters into the peridotite. The orientation of the phlogopite flakes is concordant to the lithological contacts, which are generally sharp.

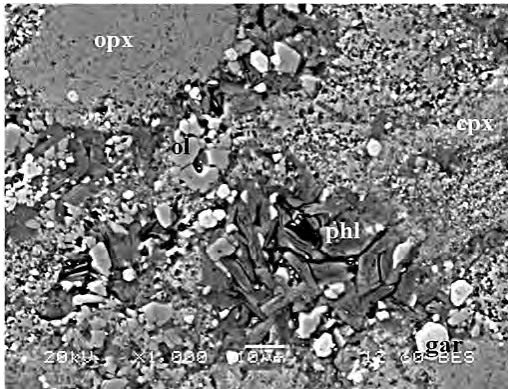


Figure 1. BSE/SE image of the run products, consisting of phlogopite, olivine, clino-pyroxene, orthopyroxene and garnet.

For this study phlogopites from garnet-amphibole harzburgite, MO10, and from amphibole harzburgite 300b, (Obata and Morten, 1987) were selected.

### Synthetic samples

Synthetic samples were synthesized by multi anvil subsolidus experiments (4.8-6.0 GPa, 680 °C) at the Experimental Petrology laboratory Università di Milano, modelling a K-doped lherzolite in the  $K_2O$ - $Na_2O$ - $CaO$ - $FeO$ - $MgO$ - $Al_2O_3$ - $SiO_2$ - $H_2O$  (KNCFMASH) system, with the phlogopite metasomatic component included as part of the starting material and not added as a separate material. The bulk composition is that of Konzett and Ulmer (1999), described in Fumagalli et al. (2009) and reported in Table 1. All experiments were carried out at fluid saturated conditions. Fluid speciation was constrained by graphite and  $H:O = 2$ . The synthesis procedure, the apparatus and the P-T conditions are largely described in Fumagalli et al., 2009.

Although textural evidences support equilibrium crystallization for phlogopites (Figure 1), further experiments have been performed with K, Al deficient compositions; a

gel with the stoichiometry of average phlogopites obtained at 4.8 GPa, 680 °C was prepared in the simplified system  $K_2O$ - $FeO$ - $MgO$ - $Al_2O_3$ - $SiO_2$ - $H_2O$ , without considering, for sake of simplicity, Na and Ca (bulk Ph11, Table 1). The deficient phlogopite composition was run at the same pressure and temperature conditions, i.e. at 4.8 GPa, 680 °C.

## Experimental

### X-ray data collection and refinements

Phlogopite from samples MO10 and 300b generally have intergrowths and stacking faults that strongly affected the crystal quality. As a consequence several crystals were checked before obtaining good X-ray diffraction data.

Single-crystal diffraction was carried out at the Dipartimento di Scienze della Terra (Università di Perugia) with a Xcalibur (Oxford Diffraction) diffractometer equipped with CCD detector, using a monochromatic  $MoK\alpha$  radiation. Data collection parameters are reported in Table 2.

Table 1. Compositions of starting materials. Klz2: "modified Brian 2 + phl1" as in Konzett and Ulmer (1999); Phl: composition of gel for phlogopite synthesis, corresponding to phlogopite phase composition produced at 4.8 GPa, 680 °C (run Klz2, Fumagalli et al., 2009).

	KLZ2	Ph11
SiO <sub>2</sub>	45.92	49.19
Al <sub>2</sub> O <sub>3</sub>	4.43	10.24
FeO	7.04	3.71
MgO	37.74	31.53
CaO	3.59	
Na <sub>2</sub> O	0.71	
K <sub>2</sub> O	0.57	5.33
Total	100.00	100.00
X <sub>Mg</sub>	0.91	0.97

Table 2. Details of single crystal X-ray refinements and geometrical parameters for natural phlogopites. Lattice parameters and bond distances are in Å. The angles are in degrees.

	MO10-1	MO10-2	300b-1	300b-2
<b>Crystal Data</b>				
<i>a</i>	5.345(2)	5.318(2)	5.312(1)	5.314(2)
<i>b</i>	9.258(2)	9.219(1)	9.219(2)	9.221(2)
<i>c</i>	10.198(3)	10.257(4)	10.293(3)	10.276(3)
$\beta$	100.15(2)	99.94(2)	100.05(2)	99.85(3)
<i>V</i>	496.74	495.32	496.33	496.15
<b>Data collection</b>				
Detector to sample distance (cm)	6.56	6.56	6.65	6.65
Measuring time (sec)	40	40	40	40
Maximum covered $2\theta$ (°)	59	59	58	66
scan mode	$\omega$	$\omega$	$\omega$	$\omega$
Collected reflections	1533	1667	1522	3055
Unique Reflections	671	438	600	903
Frame width (°)	0.7	0.7	0.7	0.7
Rint %	7.09	2.78	1.68	5.2
<b>Refinement</b>				
Refinement	Full-matrix least squares on F <sup>2</sup>			
Final $R_{obs}[F_o > 4s(F_o)]$	0.0831	0.0604	0.0265	0.0922
Number of last square parameters	62	62	62	59
<i>T-O3</i>	1.637(9)	1.639(5)	1.655(2)	1.637(3)
<i>T-O1</i>	1.668(9)	1.662(5)	1.656(2)	1.652(8)
<i>T-O2</i>	1.676(9)	1.666(3)	1.661(1)	1.662(5)
<i>T-O1</i>	1.671(9)	1.664(4)	1.659(2)	1.664(8)
< <i>T-O</i> >	1.663	1.658	1.658	1.654
<i>M1-O4</i>	2.062(13)	2.054(5)	2.050(3)	2.048(10)
<i>M1-O3</i>	2.087(8)	2.094(4)	2.086(2)	2.096(1)
< <i>M1-O</i> >	2.074	2.074	2.068	2.072
<i>M2-O4</i>	2.076(9)	2.059(5)	2.064(2)	2.064(8)
<i>M2-O3</i>	2.082(10)	2.082(5)	2.072(2)	2.082(3)
<i>M2-O3</i>	2.091(8)	2.091(4)	2.077(2)	2.091(1)
< <i>M2-O</i> >	2.083	2.078	2.071	2.079
<i>K-O1</i>	2.955(9)	2.972(4)	2.971(2)	2.974(8)
<i>K-O2</i>	3.382(13)	3.392(6)	3.382(3)	3.374(10)
$\Delta K-O$	0.428	0.42	0.412	0.408
$\Psi M1$ (°)	58.7	58.6	58.8	58.5
$\Psi M2$ (°)	58.8	58.5	58.8	58.5
$\alpha$ (°)	9.45	9.33	9.28	9.03

The intensities were corrected for Lorentz - polarization and empirical absorption correction was applied using the SADABS package (Sheldrick, 1996). Least-squares anisotropic refinements were carried out using the SHELXL-97 software (Sheldrick, 1997). Neutral scattering factors were used. Some residuals in the difference Fourier synthesis were found during the latest stage of the refinement. They can be the consequence of random stacking faults with a  $b/3$  component or a  $[310]$  microtwinning or  $2M_1$  domains in a  $1M$  dominant crystal. Thus, different scale factors for reflections with  $k \neq 3n$ , which, being affected by streaking, are systematically underestimated, were introduced as suggested by Oberti et al. (1993).

In the latest stage of the refinement a residual in the difference Fourier synthesis was found at about 0.9 Å from the O4 site and attributed to the H of the OH group. This position was then refined fixing an isotropic displacement parameter. Atomic coordinates are available from authors on request.

X-ray powder diffraction data of the run products Klz2 and Phl1 were collected with a Debye-Scherrer geometry using a capillary sample mounting. Klz2 experiments were carried out at the Dipartimento di Scienze della Terra

(Università La Sapienza, Roma, Italy) on a Instrument Siemens D5005 operating at 40 kV and 40 mA with a  $\text{CuK}\alpha$  X-ray radiation. Sample was mounted on a rotating capillary (30 r/min) and data collection was carried out with a  $0.01^\circ$  step size and 30 s counting time.

Phl1 was mounted on a capillary and collected on a Xcalibur (Oxford Diffraction) diffractometer equipped with a CCD detector, using a monochromatic  $\text{MoK}\alpha$  radiation and a routine for powder samples of the CrysAlis software. Relevant data are reported in Table 3. The powder pattern intensities were corrected for Lorentz- polarization and extracted in a GSAS format.

In Klz2 experiments all crystalline phases were identified and included in the model for a full-profile refinement using a EXPGUI-GSAS computer package (Larson and Von Dreele, 1986), as showed in Figure 2. Scale factor, background (18-term polynomial shifted Chebychev function), zero shift, peak profile and cell parameters were refined. The pseudo-Voigt profile function proposed by Thompson et al. (1987) was used to fit the experimental pattern. The asymmetry correction of Finger et al. (1994) was applied. Atomic parameters and site occupancies were refined for phlogopite.

The results of the quantitative phase analysis

Table 3. Rietveld quantitative analysis on synthetic Klz2. The lattice parameters of Klz2 minerals and Phl1 phlogopite were refined by Le Bail method.

Phases	Klz2			Phl1		
	O1	Opx	Cpx	Grt	Phl	
Wt. Fraction %	32.0	22.0	20.8	9.1	16.1	
$a$ (Å)	4.759(2)	18.24(4)	9.663(3)	11.539(2)	5.323(3)	5.290(3)
$b$ (Å)	10.213(1)	8.834(9)	8.908(3)		9.216(6)	9.271(5)
$c$ (Å)	5.987(1)	5.175(6)	5.248(2)		10.340(3)	10.153(5)
$\beta^\circ$			105.9(8)		99.97(9)	99.7(2)

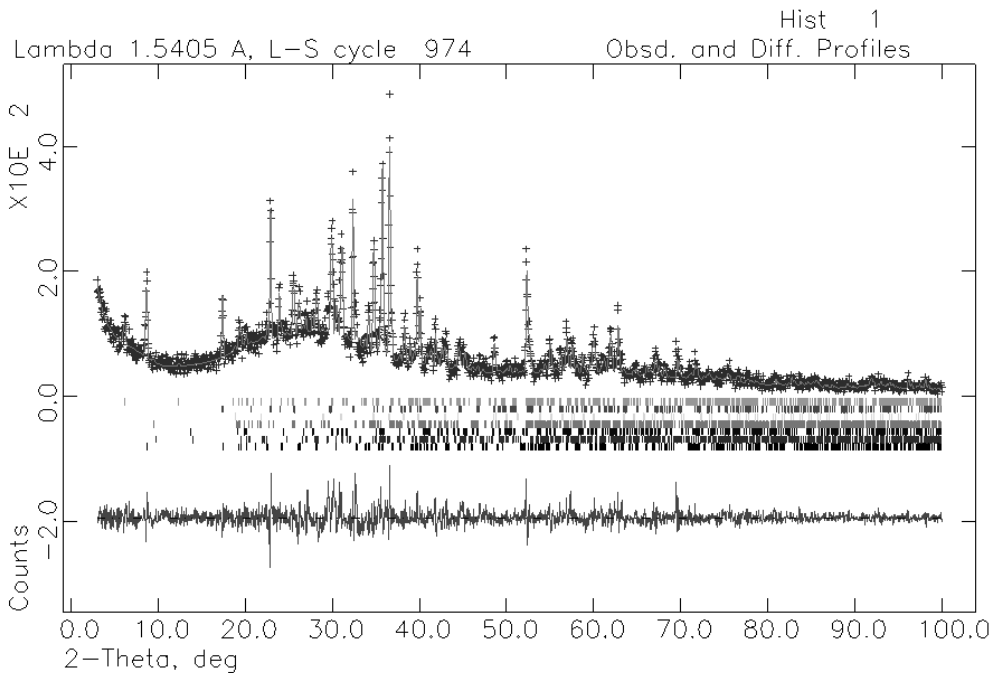


Figure 2. X-ray powder diffraction data and Rietveld refinement profile for Klz2. The solid line represents the calculated pattern obtained by the Rietveld refinement. The lower trace is a plot of the residual spectrum. The nominal position of angle for chlorite, orthopyroxene, garnet, olivine, clinopyroxene, talc, phlogopite, (from upper to lower) are reported.

are reported in Table 3. The measurement of lattice parameters were also performed using the Le Bail method (Le Bail et al., 1988). Site occupancies of phlogopite were refined by Rietveld method in the late stage of the refinements.

The same procedure as above was adopted for Ph11 powder pattern (Figure 3).

#### EMPA

Chemical compositions of the crystals used for the XRD study was determined using the Cameca SX50 of the Istituto di Geoscienze e Georisorse (Consiglio Nazionale delle Ricerche, sezione di Padova, Italy), equipped with four vertical wavelength-dispersive X-ray spectrometers and

one energy-dispersion X-ray spectrometer. The electron beam voltage and current were set to 15 kV and 10 nA, respectively, the beam was enlarged to a diameter of 5  $\mu\text{m}$ , counting times of 10 s for peak and background were used. X-ray counts were converted into oxide weight percentages using the PAP routine provided by Cameca. The results are reported in Table 4 as average over a valuable (up to 6) number of spots. No chemical zonation has been observed in these samples.

Synthetic samples have been analysed using a JEOL JXA 8200 equipped with five wavelength dispersive spectrometers (at the Dipartimento di Scienze della Terra di Milano). Phlogopites were analyzed using a 3  $\mu\text{m}$  beam at 15 kV and 5 nA

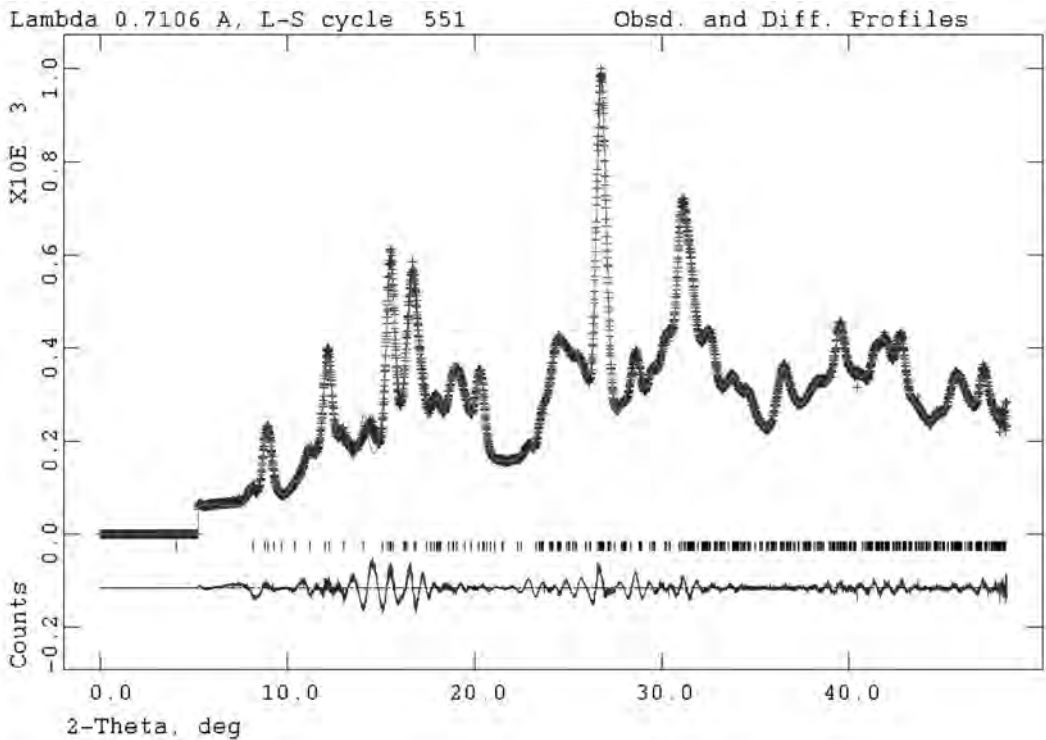


Figure 3. X-ray powder diffraction data and Le Bail refinement profile for Ph11. The solid line represents the calculated pattern obtained by refinement. The lower trace is a plot of the residual spectrum.

beam current. Natural and synthetic minerals were used as standards. All standards were calibrated within 0.5% at one standard deviation. Raw data were corrected using a Phi-Rho-Z quantitative analysis program (Table 4).

#### SIMS

The quantitative determination of Li, B, F, Cl and H, for the samples MO-10, 300b and Ph11 were carried out with a Cameca IMS 4f ion microprobe (at CNR-Istituto di Geoscienze e Georisorse (IGG), Sezione di Pavia, Italy). The primary beam consisted of mass filtered  $^{16}\text{O}^-$  and was focused on spots of 15-20  $\mu\text{m}$  in diameter at a primary current intensity typically of 10 nA. The primary accelerating voltage was -12.5 kV.

The secondary ions sputtered from polished, gold coated samples were transferred to the mass spectrometer by a nominal acceleration voltage of 4.5 kV, using the ion-imaged field of 25  $\mu\text{m}$  in diameter. Mass calibration was checked before each analysis. Quantification of the SIMS analysis was carried out using the  $\text{SiO}_2$  content as internal standard and secondary "Ion Yields" determined by means of natural and synthetic standards analyses, following Ottolini et al. (1995) and references therein. The precision of the H determination was estimated on the basis of the reproducibility of the standards analysis, resulting better than 8% relative. The overall accuracy of the volatile and light elements determination, at the concentration level

Table 4. Phlogopites chemical composition (major elements are in wt%, Li and B in ppm) recalculated on the basis of 12(OH, F, Cl), Fe<sup>2+</sup>/Fe<sup>3+</sup> ratio from Mössbauer, Cl and F are from SIMS analyses.

	<b>MO10-1</b>	<b>300b-1</b>	<b>MO10-2</b>	<b>300b-2</b>	<b>Ph11</b>
Na <sub>2</sub> O	0.44(5)	0.21(6)	0.61(9)	0.44(8)	-
MgO	25.2(2)	26.2(1)	24.8 (2)	24.6 (1)	28.8(2)
Al <sub>2</sub> O <sub>3</sub>	15.1(2)	15.7(2)	14.9(2)	15.4 (2)	6.8(2)
SiO <sub>2</sub>	39.0(3)	40.1(3)	39.6(3)	39.3 (3)	53.0(5)
K <sub>2</sub> O	8.2(1)	8.9(1)	8.0(1)	8.3(1)	4.3(2)
TiO <sub>2</sub>	1.07(4)	0.20(4)	0.98(6)	0.62(4)	-
Cr <sub>2</sub> O <sub>3</sub>	0.57(9)	0.63(8)	0.48(7)	0.6(8)	-
MnO	0.03(3)	0.04(2)	0.02(3)	0.01	-
FeO	2.73(8)	2.26(9)	2.71(7)	2.47(9)	2.53(9)
BaO	2.19(5)	0.29(4)	2.13(6)	0.56(5)	-
Fe <sub>2</sub> O <sub>3</sub>	0.37(8)	0.25(9)	0.37(7)	0.34(9)	-
H <sub>2</sub> O	3.80	4.00	3.80	4.00	4.00
F	0.11	0.09	0.12	0.16	-
Cl	0.14	0.18	0.15	0.32	-
Total	99.0	99.1	98.7	97.1	99.43
-O ≡ F, Cl	0.09	0.09	0.09	0.17	-
Li	83	43	63	43	-
B	4	5	4	2	-
Si	2.81(4)	2.83(3)	2.85(3)	2.84(3)	3.55(5)
Al	1.19(2)	1.17(1)	1.15(2)	1.16(1)	0.45(5)
Al	0.1(2)	0.14(1)	0.12(2)	0.16(1)	0.09(2)
Ti	0.06(3)	0.01(5)	0.05(4)	0.03(3)	-
Cr	0.03(1)	0.03 (1)	0.03 (9)	0.03(6)	-
Fe <sup>2+</sup>	0.16(1)	0.13(1)	0.16(1)	0.15(9)	0.14(9)
Fe <sup>3+</sup>	0.02(1)	0.01(1)	0.02(1)	0.02(9)	-
Mn	0.00 (4)	0.002(3)	0.001(2)	0	-
Mg	2.71(4)	2.77(1)	2.67(3)	2.65(4)	2.88(5)
Na	0.06(2)	0.03(1)	0.09(2)	0.06(2)	-
K	0.75(2)	0.81(2)	0.74(2)	0.77(2)	0.37(2)
Ba	0.06(1)	0.01(3)	0.06(1)	0.02(1)	-
F	0.03(1)	0.02(1)	0.03(1)	0.02(1)	-
Cl	0.02(1)	0.02(1)	0.02(1)	0.02(1)	-
OH	1.83	1.89	1.83	1.89	1.79
Sum (OH, F, Cl)	1.88	1.93	1.88	1.93	-
O <sup>2-</sup>	0.12	0.07	0.12	0.07	0.21

exhibited by the samples of this work, is better than 15% relative (Table 4).

### TEM

TEM investigations were carried out at the Dipartimento Geomineralogico of the Università di Bari with a Jeol JEM 2010. The microscope has a point to point resolution of  $\sim 2\text{\AA}$ , is equipped with a  $\pm 20^\circ$  double tilt specimen holder, an Energy Dispersive X-ray detector (EDX) for chemical analyses, and a Gatan 794 CCD camera for image acquisition.

A small amount of the experimental run Ph11 containing phlogopite crystals were powdered with agate mortar, suspended in ethanol and drop-deposited on a holey carbon film supported on a copper grid. Because of their platy habit, micas crystals tend to settle down with their (001) basal plane parallel to the carbon membrane, thus allowing observations only along  $c^*$  - or directions close to it - while the most informative directions are those disclosing the stacking sequence, i.e. at  $90^\circ$  with respect to  $c^*$ . In order to image micas also along [UV0] directions, some samples were also prepared through ultramicrotomy. Some mica crystals were embedded in a low viscosity epoxy resin, centrifuged in order to promote crystal settling, and cross sectioned with a diamond knife perpendicularly to the crystals flakes. The

recovered slices, 40-50 nm in thickness, were mounted on carbon coated copper grids and analysed at the TEM.

### MÖSSBAUER

Mössbauer spectra of the 300b and MO10 phlogopites were recorded by using a conventional constant-acceleration spectrometer, which utilizes a room temperature Rh matrix  $^{57}\text{Co}$  source, at the Dipartimento di Scienze Chimiche (Università di Padova, Italy). The isomer shift ( $\delta$ ), quadrupole splitting ( $\Delta\text{EQ}$ ), full linewidth at half maximum ( $\Gamma$ ), expressed in mm/s, were obtained by means of a standard least-squares minimisation technique. Isomer shift is quoted relative to metallic iron at room temperature. In order to avoid the iso-orientation of the phlogopite samples, the spectra were collected by using a magic angle between the sample and the  $\gamma$ -beam (Table 5 and Figure 4).

## Results

### Natural Phlogopites

The Ulten micas from garnet-amphibole harzburgite MO10 and amphibole harzburgite 300b, are 1M - phlogopites, with similar composition close to the pure end-member with low value of  $\text{TiO}_2$  (MO10: 1.07-0.98wt%; 300b:

Table 5. Mössbauer parameters: isomer shift ( $\delta$ ), quadrupole splitting ( $\Delta\text{EQ}$ ), full linewidth at half maximum ( $\Gamma$ ), for the Ulten phlogopites.

	T(K)	$\delta$ (mm/s)	$\Delta\text{EQ}$ (mm/s)	$\Gamma$ (mm/s)	A%	Attribution
<b>300b</b>	298	0.31	0.40 $\pm$ 0.10	0.60 $\pm$ 0.01	10 $\pm$ 2	$^{\text{VI}}\text{Fe}^{3+}$
		1.11 $\pm$ 0.01	2.40 $\pm$ 0.04	0.38 $\pm$ 0.04	49 $\pm$ 2	$^{\text{VI}}\text{Fe}^{2+}$
		1.13 $\pm$ 0.01	2.74 $\pm$ 0.03	0.33 $\pm$ 0.02	41 $\pm$ 2	$^{\text{VI}}\text{Fe}^{2+}$
<b>MO10</b>	298	0.31	0.45 $\pm$ 0.06	0.50 $\pm$ 0.10	12 $\pm$ 2	$^{\text{VI}}\text{Fe}^{3+}$
		1.11 $\pm$ 0.01	2.42 $\pm$ 0.01	0.35 $\pm$ 0.01	47 $\pm$ 2	$^{\text{VI}}\text{Fe}^{2+}$
		1.10 $\pm$ 0.01	2.74 $\pm$ 0.01	0.29 $\pm$ 0.01	41 $\pm$ 2	$^{\text{VI}}\text{Fe}^{2+}$

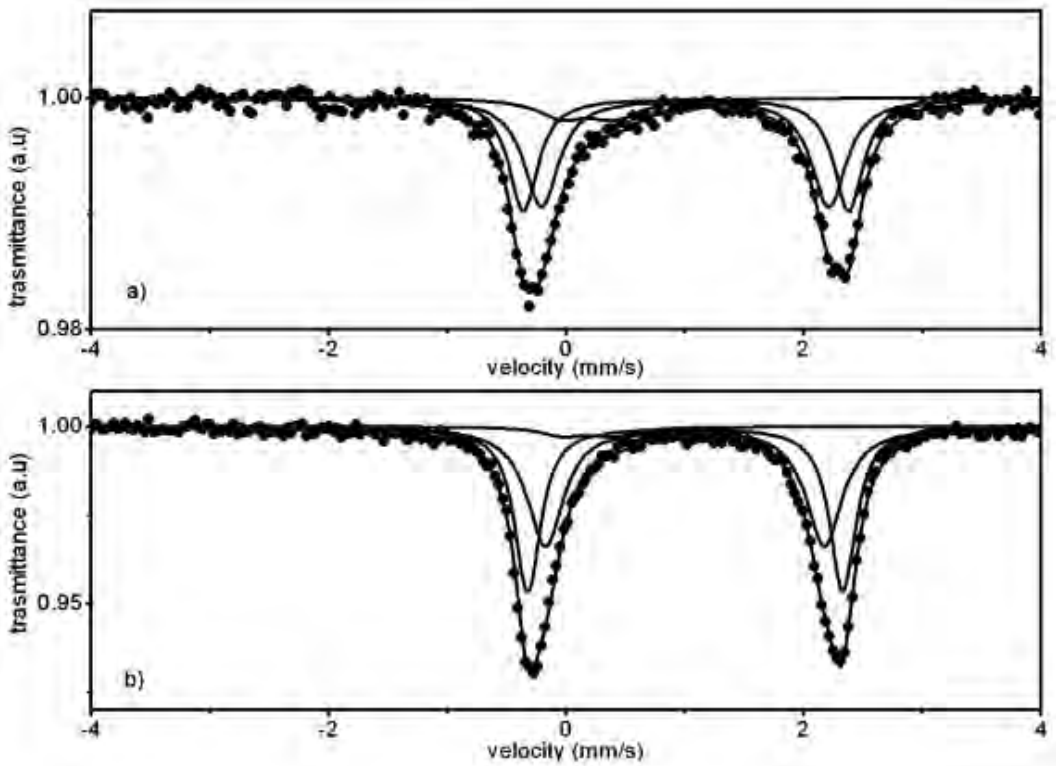


Figure 4. Mössbauer spectra of MO10(a) e 300b (b) phlogopites.

0.20-0.62wt%), FeO (MO10: 2.73-2.71wt%; 300b: 2.26-2.47wt%) Fe<sub>2</sub>O<sub>3</sub> (MO10: 0.37-0.37wt%; 300b: 0.25-0.34wt%), and high Mg# [ $100 \cdot \text{Mg}/(\text{Mg} + \text{Fe}^{2+})$ ]: 90 for MO10 and 92 for 300b. The Fe<sup>2+</sup>/Fe<sup>3+</sup> ratio was determined by room temperature (RT) Mössbauer spectroscopy. The best spectra fitting was obtained by using a minimum number of Lorentzian doublets, values are reported in Figure 4. The samples show a small absorption due to the presence of 10-12 % of octahedral Fe<sup>3+</sup>.

In both samples the interlayer A site is occupied by K (MO10: 0.75-0.74 a.p.f.u.; 300b: 0.81-0.77 a.p.f.u.) with minor substitution of Ba and Na that does not account for a full site occupancy in both samples (MO10: 0.87-0.89

a.p.f.u.; 300b: 0.85-0.85 a.p.f.u.). The values of F, Cl and OH measured by SIMS, showed only a minor substitution of Cl and F for the OH that have values close to stoichiometry (Table 4).

From a geometrical viewpoint the structure is very close to that of pure phlogopite end member, the tetrahedral rotation angle  $\alpha$  (Toraya, 1981) is about 9°, a value typical for natural phlogopites (Brigatti and Guggenheim, 2002). The tetrahedral rotation angle is the parameter that describes the distortion of the hexagonal basal oxygens ring of the tetrahedral sheet that is required in order to adjust the lateral misfit of the tetrahedral and octahedral sheets in the stacking sequence of mica.

The M1 and M2 octahedra are mainly occupied

by Mg (MO10: 2.71-2.67 a.p.f.u.; 300b: 2.77-2.65 a.p.f.u.) and resulted in a quasi-homooctahedral structure, as expected from their composition. The mean bond lengths  $\langle M1-O \rangle$  and  $\langle M2-O \rangle$  and the octahedral flattening angle ( $\Psi$ ) and the geometrical parameters are reported in the Table 2.

### *Synthetic Phlogopites*

Run products obtained in the K-doped lherzolite system at 4.8 GPa, 680 °C (Klz2) are made of olivine, clinopyroxene, orthopyroxene, garnet and phlogopite. No amphiboles were found, and the only hydrous phase present together with micas, is talc (less than 1%). Textural and chemical data of this run has been described in Fumagalli et al. (2009), within a study investigating the phase relations in metasomatised mantle compositions. Previous investigations suggest that phase assemblages are in equilibrium and that phlogopite represents an equilibrium phase as well. Results of quantitative analysis obtained by Rietveld full profile refinement are shown in Table 3.

Run products of Ph11, checked by X-ray diffractometry, resulted to be made mainly of phlogopite and trace amount of garnet, further confirming the stability of phlogopite with the peculiar mineral chemistry obtained in the K-lherzolite system at high pressure.

TEM observations confirm the synthesis of K-deficient phlogopite and contributed to further characterize the experimental run products. It has been observed that under the highly focused electron beam potassium tends to diffuse very quickly. As simple test, some crystals were analysed with the same beam intensity but different beam size on the crystal surface: by varying the electron dose per atom, a negative correlation of the K-content with the electron dose is apparent (Figure 5a).

High resolution images of the stacking sequence, although very noisy because of the notable sensitivity of these high pressure phlogopite crystals under the highly focused

electron beam, reveal a remarkable density of stacking faults (Figure 5b). Since elemental diffusion is largely augmented in the presence of crystal defects, we were aware of the possible artefacts introduced by analytical techniques based on focused electron beams. Extreme care was thus taken at the electron microprobe, monitoring the X-ray flux rate during acquisition, so that we can confidentially maintain that no elemental diffusion occurred during electron microprobe analyses.

Crystal structure refinements suggest that lattice parameters of synthetic phlogopites well compare with the lattice parameters of natural phlogopites (Comodi et al., 2004), with the exception of the *c* parameter, that has larger values respect to those of phlogopites which have the interlayer A site position completely occupied.

The *c* lattice parameters of the studied phlogopites were plotted versus the K interlayer content (Figure 6) together with those of 10 Å phase (Comodi et al., 2004), talc (Perdikatsis and Burzlaff, 1981) and phlogopite with interlayer completely occupied. The trend shows that the reduction of K occupancy increases the *c* lattice parameter and that our phlogopites samples seem to be intermediate between phlogopite and 10 Å phase. Taking into account that the stacking sequence of 10 Å phase (Comodi et al., 2004) is the same of phlogopite, differently from talc sequence, our results indicate, on a structural basis, that the “10 Å phase” component contributes to phlogopite solid solution rather than the talc-like component.

## **Discussion and conclusions**

### *Crystal chemistry and structural modifications*

Compositional variations in phlogopites can be described in terms of substitutions starting from phlogopite structural formula  $KMg_3AlSi_3O_{10}(OH)_2$  and involving i)  $MgFe_{-1}$  exchange, ii)  $KNa_{-1}$  exchange, iii)  $MgSi^{IV}Al_{-1}^{VI}Al_{-1}$  (Tschermak exchange) and  $^{XII}\square SiK_{-1}^{IV}Al_{-1}$

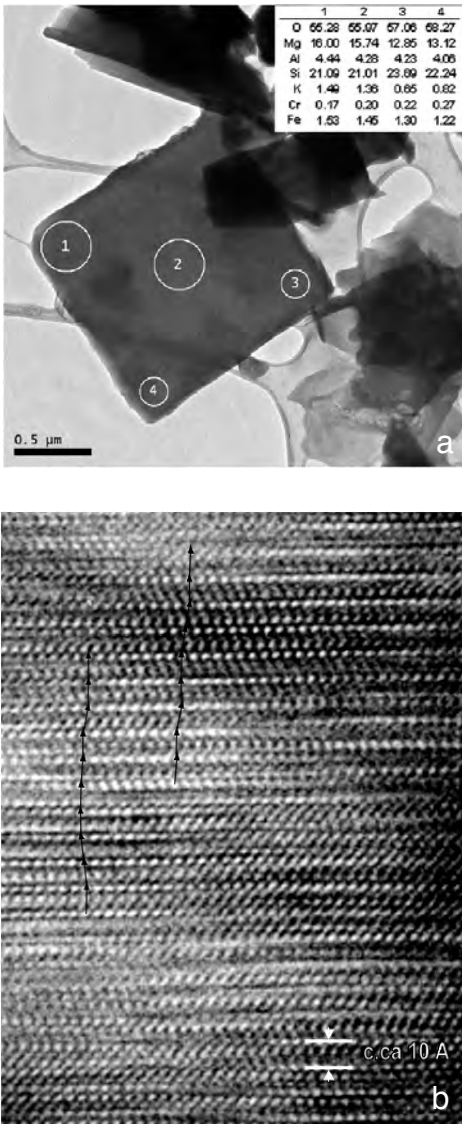


Figure 5. a: phlogopite (001) flake on a lacey carbon film. Rings represent the beam diameter on the crystal surface and the inset table reports the corresponding, internally consistent, elemental compositions (raw data, no calibration of the quantification routine was performed). b: high resolution image of the stacking sequence as seen down  $\langle 110 \rangle$ . Note the random changes in the stacking vectors (arrows) and the bending of the (001) planes.

exchange (where  $X_{II}^{\square}$  represents interlayer vacancies, K-edenite-talc exchange). The  $MgFe_{-1}$  simple cation exchange indicates an  $X_{Mg}$  comparable with mantle phlogopites, while  $KNa_{-1}$  exchange reflects the low Na content in phlogopite related to buffering effects of clinopyroxene +/- amphibole assemblages, both of which preferentially partition Na with respect to phlogopite.

Tschermak exchange vector shifts phlogopite toward eastonite component -  $KMg_{2.5}Al_{0.5}Si_{2.5}Al_{1.5}O_{10}(OH)_2$ : a decrease in aluminum down to values as low as 1 a.p.f.u. is in agreement with a decrease in eastonite component, occurring when phlogopite coexists with amphibole. Investigating felsic rocks at pressures ranging from 2.0 to 4.0 GPa and temperatures from 780 to 900 °C, Hermann (2002) found that phlogopite, at increasing pressure, preferentially forms solid solution with talc rather than phengite. The relevance of talc component in phlogopite was also suggested by Wunder and Melzer (2003), who investigated the concentration of interlayer vacancies as a function of composition in three series of synthetic phlogopite (Rb-series, Cs-series and Ba-series) at 0.2-2.0 GPa and 700-800 °C (Figure 7).

Konzett and Ulmer (1999) suggested the presence of a talc component in phlogopite produced in peralkaline KNCMASH system. Fumagalli et al. (2009) reported that in a K-doped lherzolite system, phlogopites developed at highest pressure have  $^{IV}Al < 1$  a.p.f.u. which requires  $X_{II}^{\square}SiK_{-1}^{IV}Al_1$  exchange vector to be invoked. As a result, phlogopite composition is shifted toward a talc component represented by the K-edenite exchange vector. Alternatively, the  $Al_2Mg_{-1}\square Si_2$  exchange vector (where  $\square$  represents octahedral vacancies), that leads to the Al-free tetrasilicic mica montdorite ( $KMg_{2.5}\square_{0.5}Si_4O_{10}(OH)_2$ ), might also be involved. Konzett and Ulmer (1997) interpreted phlogopites synthesized at pressure  $> 6$  GPa with  $^{IV}Al < 1$

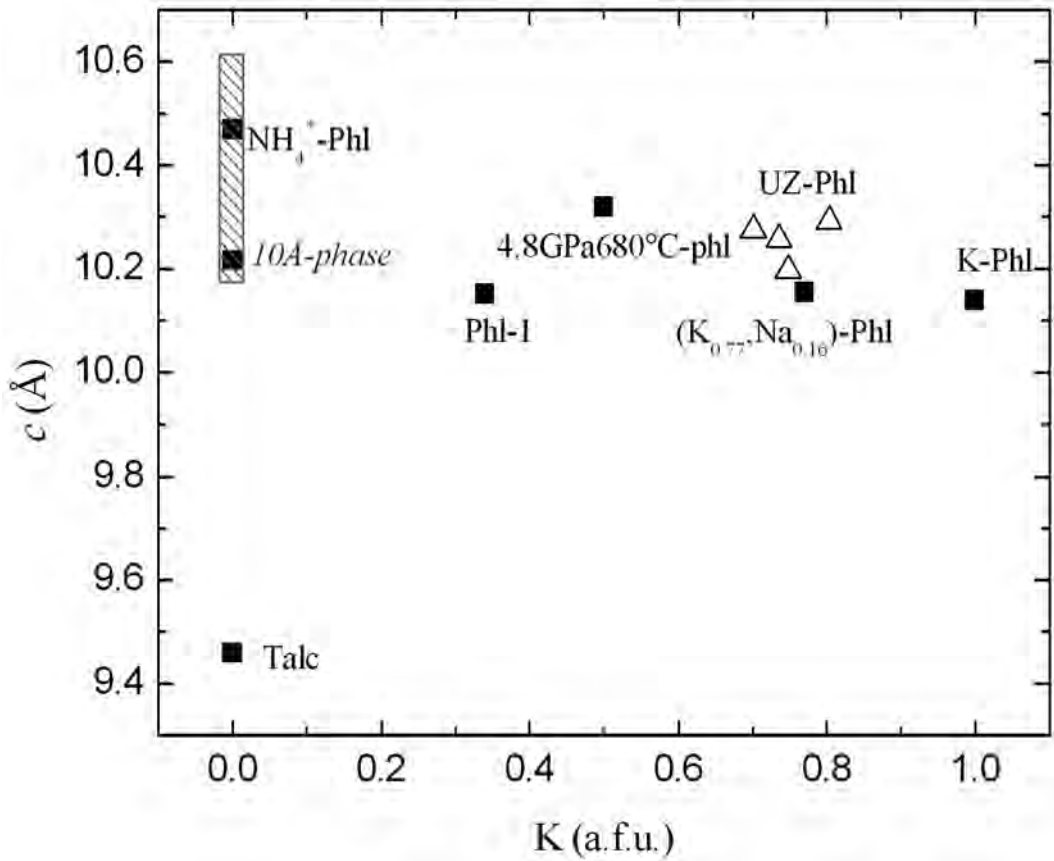


Figure 6. Evolution of *c* lattice parameter with potassium content values for the Ulten Zone samples (open triangle), synthetic 4.8 GPa-680 °C and Phl1 phlogopites, pure end-member phlogopite, NH<sub>4</sub><sup>+</sup>-phlogopite, talc and 10 Å-phase range (Comodi et al., 2005) (full squares).

a.p.f.u., as a result of montdorite component. However, as no deficiencies in octahedral cations have been recognized in the samples of the present study, this latter alternative substitution can be ruled out. Furthermore, celadonite component is negligible, suggesting any di-trioctahedral miscibility. As a result, the phlogopites of this study can be chemically described as talc-eastonite-phlogopite solid solution, while no evidences for muscovite/celadonite components have been found.

The Tschermak and talc-edenitic substitutions

produce opposite effect on tetrahedral rotation angle  $\alpha$ : whereas the Tschermak's substitution tends to increase the amount of the  $\alpha$ , the talc-edenitic substitution leads to a reduction of the tetrahedral dimension and then to a decrease of the  $\alpha$  rotation. Mercier et al. (2006) argued that the upper limit of tetrahedral rotation is equal to 9.5° for <sup>IV</sup>(AlSi<sub>3</sub>) and observed that this limit is strictly observed for all K-rich near Al-Si<sub>3</sub> tetrahedral composition in natural and synthetic samples due to an intra-tetrahedral-sheet bonding limit and to interlayer site configuration.

This implies that compositional limits are imposed in micas and element partitioning is constrained by geometrical limit. In the Ulten zone phlogopites we measured a tetrahedral aluminum content higher than one ( $Al_{1.15}Si_{2.85}$ ) and an  $\alpha$  tetrahedral rotation lower than the limit of  $9.5^\circ$  due to the talc-edenitic substitution. Moreover, in these samples the effect of combined Tschermak and talc-edenitic substitutions prevents the silica enrichment (MO10: Si:Al = 2.81:1.19; 300b:2.83:1.17), but favours the vacancy substitution for K in the interlayer (MO10: 13-11%; 300b: 15-15%).

At high pressure conditions, however, a talc

component might translate into a  $10 \text{ \AA}$  phase component, being this last phase the product of the reaction  $\text{talc} + \text{H}_2\text{O} = 10 \text{ \AA}$  phase, occurring at pressure between 4 and 5 GPa, at 600-700 °C. Really the studied samples have  $c$ -parameter in between that of phlogopite and  $10 \text{ \AA}$  phase (Figure 6), far from that reported for talc, suggesting that the  $10 \text{ \AA}$  phase might represent the end member of this coupled substitution.

Comodi et al. (2004), studying the high pressure behaviour of phlogopite, showed that the  $\alpha$  tetrahedral rotation increases with pressure due to the higher compressibility of the octahedral layer with respect the tetrahedral

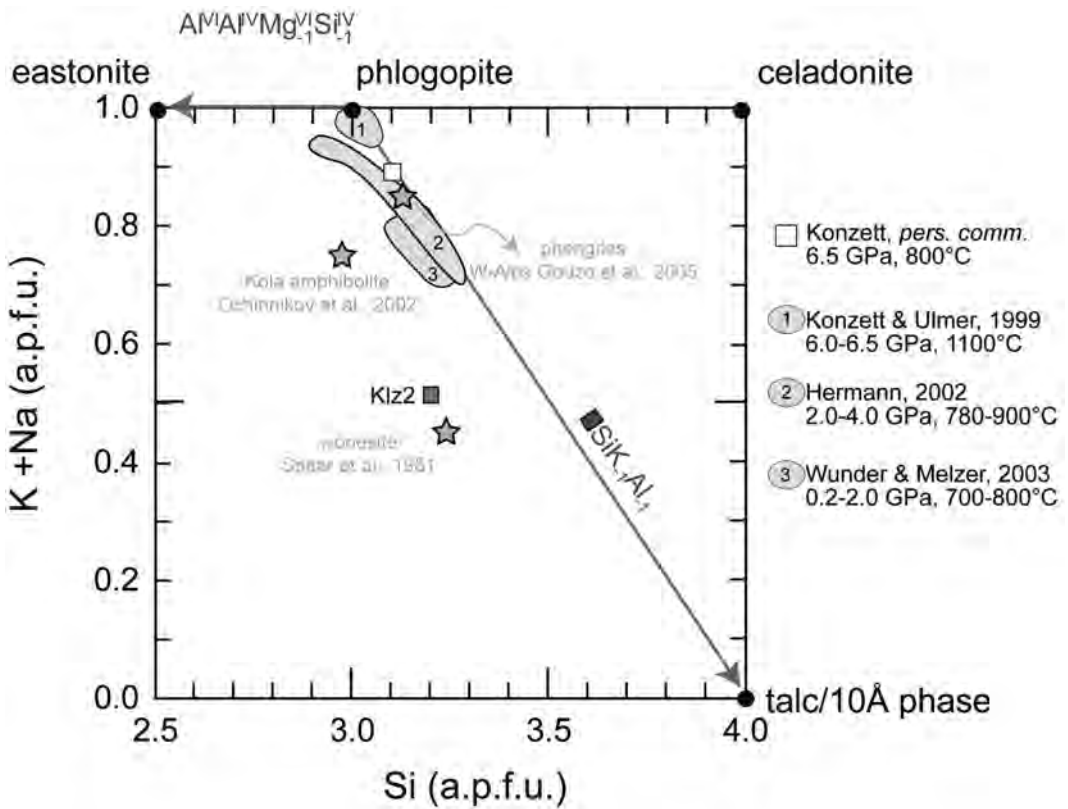


Figure 7. Mineral-chemistry of studied phlogopites compared with previous experimental data (Konzett and Ulmer, 1999; Hermann, 2002; Wunder and Melzer, 2003). Symbols: open triangles: Ulten phlogopites; full square Klz2.

layer. The edenitic substitution,  $K + Al = X_{II} \square + Si$ , producing a decrease of the  $\alpha$  angle, counterbalances the effect of a pressure increase. Thus we conclude that this substitution, with a 10 Å phase component instead of a talc component, could extend the baric stability of mica reducing the  $\alpha$  tetrahedral rotation and increasing the pressure range to reach the upper tetrahedral rotation limit, although the extent of the solid solution between the phlogopite and 10 Å phase is not yet completely defined.

### Geochemical considerations

The Ulten Zone peridotites record two distinct metasomatic events that were resolved by studying the trace-element signature and the Li/Be ratio of peridotitic clinopyroxene (Scambelluri et al., 2006). The first metasomatic event was melt-induced and possibly occurred in pre-Variscan times (Petrini and Morten, 1993). The second event was fluid-induced and related to the interaction between peridotite and H<sub>2</sub>O-rich fluids, during the pressure peak of the Variscan orogeny, dated about 330 Ma, when the crystallization of amphibole and phlogopite occurred. The geochemical signature of these two metasomatic events suggest that the Ulten wedge peridotites were percolated first by melts and then by fluids, adding recycled components likely sourced from a similar crustal reservoir. Trace elements signatures are often reported for anhydrous phases assemblages of metasomatic peridotites, and the same is for amphiboles. Less often volatiles trace elements (i.e. Li, B, Be, H) are measured in hydrous phase, and very rarely on metasomatic phlogopites.

SIMS analysis of phlogopite from the Ulten peridotites show that Li varies from 43 to 83 ppm and B from 2 to 5 ppm in the MO10 and 300B peridotite respectively (Table 4). 300B peridotite has Li values of 1.82 ppm on orthopyroxene, 4.79 ppm in olivine, 5.54 ppm in amphibole and 42 ppm in phlogopite (measured by LA-ICP-MS Scambelluri et al., 2006). These values well

compare with our SIMS data.

How these elements partitioned among the phases assemblage of this metasomatic peridotite is still unknown, especially for the hydrous silicates. More data on the volatiles elements content of the Ulten peridotites phases will help to constrain the partitioning between the metasomatic fluids and minerals and to better understand the metasomatic processes.

### Acknowledgments

Thanks to A. Zanetti for the SIMS analysis and useful discussions, to L. Nodari for the Mössbauer analysis and to P. Ballirano for the powder XRD data collection on synthetic sample. Thanks to the careful reviews of Emanuela Schingaro, Cristina Perinelli and of the editor Gianni Andreozzi, which provided insights that helped to improve the paper. This work was financially supported by the Italian M.U.R.S.T grant "Vincoli Naturali (Ulten zone) e sperimentali sul ruolo delle fasi idrate nei processi di interazione crosta-mantello" to P.C.

### References

- Brigatti M.F. and Guggenheim S. (2002) - Mica crystal chemistry and the influence of pressure, temperature, and solid solution on atomistic models. In: Mottana A., Sassi F.P., Thompson J.B.Jr, Guggenheim S. (eds). *Micas: Crystal Chemistry and Metamorphic Petrology. Reviews in Mineralogy and Geochemistry*, Mineralogical Society of America and Geochemical Society, 46, 1-100.
- Comodi P., Mellini M. and Zanazzi P.F. (1990) - Scapolites: Variation of structure with pressure and possible role in the storage of fluids. *European Journal of Mineralogy*, 2, 195-202.
- Comodi P., Fumagalli P., Montagnoli M. and Zanazzi P.F. (2004) - A single-crystal study on the pressure behavior of phlogopite and petrological implication. *American Mineralogist*, 89, 647-653.
- Comodi P., Fumagalli P., Nazzareni S. and Zanazzi P.F. (2005) - The 10 Å phase: Crystal structure from single-crystal X-ray data. *American Mineralogist*, 90, 1012-1016.
- Finger L.W., Cox D.E. and Jeapcoat A.P. (1994) - A correction for powder diffraction peak asymmetry

- due to axial divergence. *Journal of Applied Crystallography*, 27, 892-900.
- Fumagalli P., Zanchetta S. and Poli S. (2009) - Alkali in phlogopite and amphibole and their effects on phase relations in metasomatized peridotites: a high pressure study. *Contributions to Mineralogy and Petrology*, 158, 723-737.
- Godard G., Martin S., Prosser G., Kienast J.R. and Morten L. (1996) - High-pressure granulites and enclosed garnet-peridotites of the Austroalpine Ulten zone: a deep fragment of the Variscan belt in the Italian Eastern Alps. *Tectonophysics*, 259, 313-341.
- Gouzo C., Itaya T. and Takeshina H. (2005) - Interlayer cation vacancies of phengites in calcshists from Piemonte zone, Western Alps, Italy. *Journal of Mineralogical Sciences*, 100, 143-149.
- Hermann J. (2002) - Experimental constraints on phase relations in subducted continental crust. *Contributions to Mineralogy and Petrology*, 143, 219-235.
- Konzett J. and Ulmer P. (1999) - The stability of hydrous potassic phases in lherzolitic mantle: an experimental study to 9.5 GPa in simplified and natural bulk compositions. *Journal of Petrology*, 40, 629-652.
- Kushiro I. (1970) - Stability of amphiboles and phlogopite in the upper mantle. *Carnegie Institute Yearbook*, 68, 245-47.
- Kushiro I., Syono Y. and Akimoto S. (1967) - Stability of phlogopite at high pressures and possible presence of phlogopite in the Earth's upper mantle. *Earth and Planetary Science Letters*, 3, 197-203.
- Larson A.C. and Von Dreele R.B. (1986) - GSAS. General structure analysis system. Report LAUR-86-748 Los Alamos National Laboratory.
- Le Bail A., Duroy H. and Fourquet J.L. (1988) - Ab-initio structure determination of  $\text{LiSbWO}_6$  by X Ray Powder diffraction. *Material Resource Bulletin*, 23, 447-452.
- Luth R.W. (1997) - Experimental study of the system phlogopite diopside from 3.5 to 17 GPa. *American Mineralogist*, 82, 1198-1209.
- Mercier P.H.J., Rancourt D.G., Rehammer G.J., Lalonde A.E., Robert J.L., Bermnan R.G. and Kodama H. (2006) - Upper limit of the tetrahedral rotation angle and factors affections octahedral flattening synthetic and natural 1M polytype C2/m space group micas. *American Mineralogist*, 91, 831-849.
- Modreski P.J. and Boettcher A.L. (1973) - Phase relationship of phlogopite in the system  $\text{K}_2\text{O-MgO-CaO-Al}_2\text{O}_3\text{-SiO}_2\text{-H}_2\text{O}$  to 35 kilobars: a better model for micas in the interior of the Earth. *American Journal of Science*, 273, 385-414.
- Morten L. and Obata M. (1990) - Rare earth abundances in the eastern Alpine peridotites, Nonsberg area, northern Italy. *European Journal of Mineralogy*, 2, 643-653.
- Obata M. and Morten L. (1987) - Transformation of spinel lherzolite to garnet lherzolite in ultramafic lenses of the Austridic crystalline complex, Northern Italy. *Journal of Petrology*, 28, 599-623.
- Oberti R., Ungaretti L., Tlili A., Smith D.C. and Robert J.L. (1993) - The crystal structure of preiwekite. *American Mineralogist*, 78, 1290-1298.
- Ottolini L., Bottazzi P., Zanetti A. and Vannucci R. (1995) - Determination of hydrogen in silicates by Secondary Ion Mass Spectrometry. *The Analyst*, 120, 1309-1314.
- Ovchinnikov N.O., Nikitina L.P., Babashkina M.S., Yakovleva A.K., Yakovlev Yu.N., Chernova O.G. and Redfern S.A.T. (2002) - Structural states of micas in amphibolites of the KSDB-3 deep borehole and their surface equivalents. *Mineralogical Magazine*, 66, 491-512.
- Pawley A.R. and Wood B.J. (1995) - The high pressure stability of talc and 10 Å phase: potential storage sites for  $\text{H}_2\text{O}$  in subduction zones. *American Mineralogist*, 80, 998-1003.
- Perdikatsis B. and Burzlaff H. (1981) - Strukturverfeinerung am talk  $\text{Mg}_3[(\text{OH})_2\text{Si}_4\text{O}_{10}]$ . *Zeitschrift für Kristallographie*, 156, 177-186.
- Petrini R. and Morten L. (1993) - Nd-isotopic evidence of enriched lithospheric domains: an example from the Nonsberg area, eastern Alps. *Terra Abstract supplement to Terra Nova*, 4, 19-20.
- Poli S. and Schmidt M.W. (2002) - Petrology of subducted slabs. *Annual Review of Earth and Planetary Sciences*, 30, 207-235.
- Scambelluri M., Hermann J., Morten L. and Rampone E. (2006) - Melt- versus fluid-induced metasomatism in spinel to garnet wedge peridotites (Ulten Zone, Eastern Italian Alps): clues from trace element and Li abundances. *Contributions to Mineralogy and Petrology*, 151, 372-394.
- Sheldrick G.M. (1996) - SADABS. Program for empirical absorption correction of area detector data. Institut für Anorganische Chemie, University

- of Göttingen, Germany.
- Sheldrick G.M. (1997) - SHELX-97. Program for crystal structure determination. University of Göttingen, Germany.
- Spear F.S., Hazen R.M. and Rumble DIII (1981) - Wonesite: a new rock-forming silicate from the Post Pond Volcanics, Vermont. *American Mineralogist*, 66, 100-105.
- Sudo A. and Tatsumi Y. (1990) - Phlogopite and K-amphibole in the upper mantle: implication for magma genesis in subduction zones. *Geophysical Research Letters*, 17, 29-32.
- Thompson P., Cox D.E. and Hastings J.B. (1987) - Rietveld refinement of Debye-Scherrer synchrotron X-ray data from  $Al_2O_3$ . *Journal of Applied Crystallography*, 20, 79-83.
- Toraya H. (1981) - Distortions of octahedra and octahedral sheets in 1M micas and the relation to their stability. *Zeitschrift für Kristallographie*, 157, 173-190.
- Trønnes R.G. (2002) - Stability range and decomposition of potassic richterite and phlogopite end members at 5-15 GPa. *Mineralogy and Petrology*, 74, 129-148.
- van Roermund H.L.M., Carswell A.D., Drury H. and Hejborer T.C. (2002) - Microdiamond in a megacrystic garnet websterite pod from Bardane on the island of Fjortoft, Western Norway: evidence for diamond formation in mantle rocks during deep continental subduction. *Geology*, 30, 959-962.
- Wunder B. and Melzer S. (2003) - Interlayer vacancy characterization of synthetic phlogopitic micas by IR spectroscopy. *European Journal of Mineralogy*, 14, 1129-1138.
- Zheng J.P., Zhang R.Y., Griffin W.L., Liou J.G. and O'Reilly S.Y. (2005) - Heterogeneous and metasomatized mantle recorded by trace elements in minerals of the Donghai garnet peridotites, Sulu UHP terrane, China. *Chemical Geology*, 221, 243-259.

*Submitted, October 2010 - Accepted, January 2011*